Int. J. Heat Mass Transfer. Vol. 35, No. 12, pp. 3275–3289, 1992
Printed in Great Britain

0017-9310/92 \$5.00+0.00

Composite expansions on forced convection over a flat plate with an unheated starting length

S. W. MA, F. M. GERNER and Y. G. TSUEI
Department of Mechanical, Industrial and Nuclear Engineering, University of Cincinnati, OH 45221-0072, U.S.A.

(*Received* 1 *October* 1991 *and in final form* 10 *February* 1992)

Abstract—The elliptic energy equation for steady, two-dimensional incompressible flow over a flat plate with an unheated starting length is analyzed using matched asymptotic expansions where the boundary layer solution has been treated as the outer expansion corresponding to the leading-edge equation as the inner expansion. It has been revealed that the linear velocity profile of flow occurs near the leading-edge of the heated part of the plate. This new technique for solving elliptic-to-parabolic equations involves stretching two different scales for two independent variables in the inner expansion. Results are applicable to the region where boundary layer theory breaks down, which is particularly interesting in microscale heat transfer.

1. INTRODUCTION

SITUATIONS arise in contemporary microelectronic and microstructure design which are beyond the limits of classical boundary layer theory as first conceived by Prandtl in 1904. An example is a micro sensor used to measure air flow [1]. Although a conventional hydrodynamic boundary layer may be formed; if the heated section is small enough, the thickness of the 'thermal boundary layer' may be equal to or even larger than the characteristic length of the heated element. However, since there is no effective non-boundary layer method available, von Kármán integral methods are still being extensively utilized [2]. As early as the late 1940s, it had been noticed that the boundary-layer solutions are the first approximations to the Navier–Stokes equations including the energy equation. Since then, many attempts have been made to obtain higher-order approximations for these equations in order to extend the solutions to lower Reynolds number flows or small length scale models. This search has led to the development of modern singular perturbation theory.

The first monograph on the perturbation method devoted to fluid mechanics was written by Van Dyke [3] in 1964. A comprehensive review, at that time, for heat transfer applications appeared in 1969 [4]. In the same paper, Van Dyke predicted that the leading-edge problem is more complicated for free convection. However, this problem has recently been solved by Pop *et al.* [5] and Martynenko *et al.* [6] with the aid of the method of matched asymptotic expansions, together with a deformed longitudinal coordinate. The key point is that for free convection the momentum and thermal boundary layers begin at the same point. Their investigations concentrated on matching the outer and inner expansions of the momentum equation. The singularity at the leading-edge of the thermal boundary layer is automatically removed.

For forced convection over a flat plate with an unheated starting length, the momentum and thermal boundary layers have different origins, one of them is at $x = -x_0$, the other at $x = 0$ (see Fig. 1). For simplicity, in this paper it is assumed that the flow at the beginning of the heated section has a Reynolds number high enough that higher-order approximations of the momentum equations are unnecessary (i.e. the standard momentum boundary layer equations are used). In other words, only the higher-order approximations of the energy equation will be considered. The entire energy equation for two-dimensional steady flow of an incompressible viscous fluid with an initially uniform temperature past a flat plate is described with an elliptic-to-parabolic equation in the intervals $-\infty < x < \infty$ and $0 \leqslant y < \infty$

$$\varepsilon\theta_{xx} + \theta_{yy} = \theta_x - \theta_y \tag{1}$$

where ε denotes a small parameter and the subscripts stand for partial differentiation with respect to the variable indicated. In this paper, equation (1) is solved with suitable boundary conditions. The detailed derivations of the energy equation with form (1) can be found in Section 2.

In the first approximation, the term involving ε is neglected. The remainder of the equation is a parabolic partial differential equation. Since the boundary conditions on the plate depend on an independent variable, x, a nonsimilarity equation results from using the Blasius similarity transformation. A historical review for nonsimilar flows before 1970 is given by Cheema [7]. Chao and Cheema [8] developed a series solution for nonsimilarity equations in wedge

NOMENCLATURE

Ai	Airy function
f	function in the Blasius equation (5)
h	heat transfer coefficient [W m^{-2} K^{-1}]
$H(x-a)$	Heaviside unit function defined by $H(x-a) = 0$ when $x < a$; and $H(x-a) = 1$ when $x > a$
I_v	modified Bessel function of the first kind with parts v
k	thermal conductivity [W m^{-1} K^{-1}]
Nu_x	local Nusselt number, hx/k
O	order symbol
Pr	Prandtl number, v/α
Re	Reynolds number on unit length, U_∞/v
Re_x	local Reynolds number, $U_\infty x/v$
T	temperature [K]
T_w	temperature of heated elements [K]
T_∞	temperature of upstream [K]
x, y	dimensionless Cartesian coordinates, outer variables for elliptic equations
x_0	dimensionless length of the unheated part, as a unit length in this paper
X, Y	inner variables for elliptic-to-parabolic equations
u	dimensionless velocity along x-direction
U_∞	velocity of upstream [m s^{-1}]
v	dimensionless velocity along y-direction.

Greek symbols

α	thermal diffusivity [m^2 s^{-1}]
δ	Dirac delta function defined by $\int_{-\infty}^{\infty} \delta(x)\,dx = 1$
ε	small parameter in differential equations, $1/\sqrt{(Re)}$
ϕ_x, ϕ_∞	functions defined in this paper, expression (37)
$\theta, \Theta, \hat{\Theta}$	dimensionless temperature defined by $(T-T_\infty)/(T_w-T_\infty)$
θ	outer expansion for elliptic equations
Θ	inner expansion for elliptic equations and outer expansion for elliptic-to-parabolic equations
$\hat{\Theta}$	inner expansion for elliptic-to-parabolic equations
v	kinematic viscosity [m^2 s^{-1}]
ψ	stream function
η	inner variable for elliptic equations and outer variable for elliptic-to-parabolic equations

Superscripts

$+$	$x \to a^+$ is equal to $a + \lim_{x\to 0} x$, where $x > 0$
$-$	$x \to a^-$ is equal to $a - \lim_{x\to 0} x$, where $x > 0$
c	composite expansion
i	inner expansion
int	integral methods.

flow with a second-stage similarity transformation. They concluded that there is no solution in closed form except for the first two terms in the series. Theoretically, a local nonsimilarity technique, due to Sparrow *et al.* [9, 10], is suitable for nonsimilarity equations. In practice, however, it is not possible to express higher-order derivatives of a discontinuous function in terms of classic primary functions. More recently, Zubair and Kadaba [11] introduced a group transformation method for unsteady mixed convection. That is, the original partial differential equations can be substituted with a set of ordinary differential equations after many transformations. In general, however, the set of equations has to be reevaluated for each time and x-location except for a few very special cases. If a closed form solution is not found for the nonsimilarity equations, obtaining higher order approximations with perturbation techniques will be difficult since it is a tedious assignment to solve a set of parabolic equations numerically even with high speed computers. In Section 3, the parabolic equation is transformed into a set of ordinary differential equations with transforms slightly different from Chao and Cheema [8]. Then special solutions are assumed so

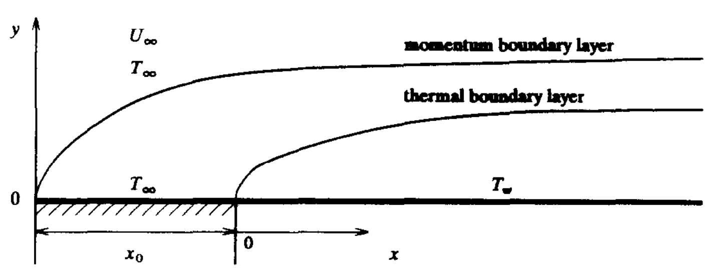

FIG. 1. Forced convection over a flat plate with an unheated starting length.

that those ordinary differential equations are transformed into a set of algebraic equations solved with a FORTRAN program of 30 statements.

After the first approximation is substituted into the term θ_{xx} in equation (1), the second approximation, which is the solution of a nonhomogeneous parabolic equation, can be obtained by the technique described above. However, it can be shown that the solution is more singular than the first as $x \to 0$. Although it is possible to move the singularity of the secular term to left of $x = 0$ with Lighthill's technique, that is, the PLK method [3], it does not make any sense in this physical situation. The source of nonuniformities is that equation (1) has the form of a small parameter multiplying the highest derivative with respect to x. The first approximation involves the loss of one boundary condition in the x-direction so that the solution does not satisfy all of the boundary conditions.† For higher approximations, a singularity at $x = 0$ might be removed with Lighthill's technique, but unfortunately, the lost boundary condition still cannot be satisfied. As pointed out by Nayfeh [12], the method of multiple scales can be applied to problems which can be or cannot be treated by Lighthill's technique and the method of matched asymptotic expansions. However, the determination of the different scales in equation (1) is complicated.

In terms of the principle of least degeneracy in matched asymptotic expansions [3], the inner expansion of equation (1) is obtained by stretching the independent variable $x = \varepsilon X$

$$\Theta_X = \Theta_{XX} \tag{2}$$

where Θ is a function of X and y. This transform is subject to deficiencies on several points. First, the solution of equation (2) exponentially convergences for $X < 0$ so that it satisfies the lost boundary condition. It does not, however, decrease for $X > 0$. Therefore, it is impossible to match with the outer solution. If the boundary conditions were defined in a finite interval, Nayfeh [12] has shown that for ordinary differential equations, equation (2) is uniformly valid near the neighborhood of x_2 for a finite interval $x_1 \leqslant x \leqslant x_2$. In other words, the location of the boundary layer occurs as $x \to x_2$. The same conclusion recently has been reported for elliptic-to-parabolic equations by Lagerstrom [13]. The situation is different, however, if the domain of x is infinite which is often the case for fluid dynamics and convection heat transfer. Only if x approaches zero, is it possible for the term θ_{xx} in equation (1) to be of the same order as the other terms. This implies that the location of the boundary layer is near the point $x = 0$, i.e. it is an internal boundary layer. Therefore, although equation (2) might be a valid inner expansion for a finite interval, it cannot be applied to infinite situations. For these problems, it is obvious that the principle of least degeneracy must be generalized.

The generalized principle of least degeneracy developed in this paper states that both of the highest derivatives and at least another term in the elliptic-to-parabolic equation (1) should be kept in the inner expansion so that the solution will exponentially decay along all directions. The reason why the highest derivative with respect to y cannot be neglected was explained in the previous paragraph. If the terms on the right-hand side of equation (1) are neglected in the inner expansion, it leads to Laplace's equation. Its general solution will be $\theta(x \pm iy)$ or $\theta(y \pm ix)$, which denotes that there is no exponential decay along at least one (x or y) direction. The technique introduced here may be traced to the initial work on the birth of boundary layers by Grasman [14] and Eckhaus [15]. With this principle, two different scales, $x = \varepsilon^{\alpha} X$, and $y = \varepsilon^{\beta} Y$, for stretching two independent variables have been proposed in the inner expansion of equation (1). This yields two algebraic equations for determining the indices α and β of ε. It is very interesting to note that the linear velocity profile of flow can be derived directly from the inner expansion. The detailed process has been included in Section 2. The partial differential equation corresponding to the shear flow will be solved with Fourier transforms in Section 4.

2. BASIC GOVERNING EQUATIONS AND MATCHED ASYMPTOTIC EXPANSIONS

The problem considered here corresponds to a finite or semi-finite flat plate under steady incompressible two-dimensional flow with an unheated starting length x_0 in the rectangular Cartesian coordinate system (x, y). Suppose that the upstream has a constant velocity U_∞ and temperature T_∞. Since the stream function may be defined by $\psi = \varepsilon\sqrt{(2(x+x_0))} f(\eta)$, the components of dimensionless velocity are

$$u = \psi_y = f_\eta, \quad v = -\psi_x = -\varepsilon(f - \eta f_\eta)/\sqrt{(2(x+x_0))} \tag{3}$$

where

$$\eta = y/\varepsilon\sqrt{(2(x+x_0))} \quad \text{and} \quad \varepsilon = 1/\sqrt{(Re)} \tag{4}$$

$Re = U_\infty/\nu$, which is much larger than one, denotes Reynolds number based on a unit length. It should be stressed that equation (4) is the well-known Blasius similarity transformation based on the boundary layer theory due to Prandtl. The first-order approximation of the momentum equations can be simplified into the Blasius equation [3]

$$f_{\eta\eta\eta} + f f_{\eta\eta} = 0. \tag{5}$$

With no-slip conditions on the plate and an upstream condition which may be formulated by $f(0) = f_\eta(0) = 0$, and $f_\eta(\infty) = 1$, the solution of equation (5)

† It will be shown in Section 3 that the omitted boundary condition is at $x \to -\infty$.

can be written as Weyl's expansion [16]

$$f = \sum_{n=0}^{\infty} (-1)^n D_n \eta^{3n+2} \tag{6a}$$

where D_n satisfies the expressions

$$(3n+2)(3n+1)3nD_n = \sum_{i=0}^{n-1} (3i+2)(3i+1)D_i D_{n-1-i}$$

$$2D_0 = 0.469600. \tag{6b}$$

The dimensionless energy equation for steady two-dimensional flow of an incompressible viscous fluid with constant temperature and small Mach number past a flat plate is

$$Pr\, u\theta_x + Pr\, v\theta_y = \varepsilon^2(\theta_{yy} + \theta_{xx}). \tag{7}$$

The appropriate boundary conditions in the Cartesian coordinate system are

$$\theta(x, y) = H(x), \quad y = 0; \tag{8}$$

$$\theta(x, y) = 0, \quad y \to \infty; \tag{9}$$

$$\theta(x, y) = 0, \quad x \to -\infty; \tag{10}$$

$$\theta_x(x, y) = 0, \quad x \to \infty;\ y > 0 \tag{11}$$

where Pr denotes Prandtl number and $H(x)$ the Heaviside unit function. It is the purpose of this paper to deal with governing equation (7) subject to boundary conditions (8)–(11) with the method of matched asymptotic expansions. The outer expansion of the elliptic equation (7) can be derived by neglecting the terms containing the small parameter, ε

$$u\theta_x + v\theta_y = 0. \tag{12}$$

Equation (12) is homogeneous with a constant temperature in the upstream which is similar to inviscid flow in the momentum equations, thus its solution has been proven to be $\theta = 0$ [17]. Because the highest derivatives are lost in the outer expansion (12), the solution is incorrect near the plate, i.e. boundary condition (8) is not satisfied.

In order to obtain a uniformly valid solution near the plate, Prandtl simplified the Navier–Stokes equations by stretching an independent variable, $y = \varepsilon Y$. His procedure, which he based on physical intuition, is known as boundary layer theory. In modern perturbation theory, this method has been named the inner expansion and has been mathematically proven by Van Dyke [3]. The boundary layer theory is also applicable to the energy equation (7) based on the fact that the highest derivatives are multiplied by a small parameter which is similar to the Navier–Stokes equations. However, it should be noted that since the boundary condition (8) depends upon the x-direction, the solution of the inner expansion is also a function of x. Therefore, with the same transformation (4) and using expression (3) to transform u and v, equation (7) can be changed into the elliptic-to-parabolic equation

$$\Theta_{\eta\eta} + f\, Pr\, \Theta_\eta - 2(x+x_0)PR\, f_\eta \Theta_x = -\varepsilon^2 \left[2\Theta_{xx}(x+x_0) + \frac{\eta^2\Theta_{\eta\eta}}{2(x+x_0)} + \frac{3\eta\Theta_\eta}{2(x+x_0)} - 2\eta\Theta_{\eta x} \right] \tag{13}$$

where $\Theta = \Theta(x, \eta)$ shows that one of its independent variables has been stretched. It is obvious that by neglecting the terms in equation (13) which include the small parameter ε, the equation will degenerate into a parabolic equation in the x-direction. Since the solution of this parabolic equation satisfies the boundary condition at the plate, it is much better than the outer expansion (12). Assuming that the dimensionless temperature Θ can be expanded in the form

$$\Theta(x, \eta) = \Theta_1(x, \eta) + \varepsilon^2\Theta_2(x, \eta) + O(\varepsilon^4) \tag{14}$$

(where the order symbol O denotes the smaller high-order terms), equation (14) can be substituted into the governing equation (13) and equating like powers of ε yields a set of iterative equations

$$\varepsilon^0: \quad \Theta_{1_{\eta\eta}} + f\, Pr\, \Theta_{1_\eta} - 2(x+x_0)Pr\, f_\eta \Theta_{1_x} = 0; \tag{15}$$

$$\varepsilon^2: \quad \Theta_{2_{\eta\eta}} + f\, Pr\, \Theta_{2_\eta} - 2(x+x_0)Pr\, f_\eta \Theta_{2_x} = -2\Theta_{1_{xx}}(x+x_0) - \frac{\eta^2\Theta_{1_{\eta\eta}}}{2(x+x_0)} - \frac{3\eta\Theta_{1_\eta}}{2(x+x_0)} + 2\eta\Theta_{1_{\eta x}}. \tag{16}$$

Equation (15) is the familiar nonsimilarity boundary layer equation which is the first-order inner approximation corresponding to the original elliptic equation (7). Equation (16) is the second-order inner approximation. According to the iterative process, the problem seems to be totally solved. However, since equation (15) is parabolic, a boundary condition along the x-direction is still lost. Although the accuracy of the solution will be increased along the surface of the plate if the higher-order approximation (16) is included, the lost boundary condition still cannot be satisfied. Following the same idea as Prandtl, it is found that when x is of order ε^2, the orders of the two sides of equation (13) are similar. This implies that the solution from boundary layer theory has become invalid near the leading-edge of the heated part of the plate. Previously, this phenomenon has not been quantitatively verified. On the other hand, it is not difficult to show that if the solution of equation (15) is singular at $x = 0$, the solution from equation (16) is more singular at the same point. Although Kuo [18] attempted to move a similar singularity in the momentum equations with Lighthill's technique, this method will fall here. For instance, assume that the singularity at $x = 0$ is moved to the left. Since the governing equation (7) is linear, superposition can be applied to predict the heat transfer for any arbitrarily specified plate temperature. In the case of a finite heated plate, singularities will occur within part of the plate. This is physically inconsistent.

Boundary layer theory offers a clue to finding a uniformly valid solution near the leading-edge. For this purpose, the concept of a boundary layer inside the conventional boundary layer is introduced. The conventional boundary layer solution is treated as the outer expansion of equation (13), which is uniformly valid along the surface of the plate except for the region near the leading-edge. The inner expansion might be found by stretching the independent variable, $x = \varepsilon^{\alpha} X$, where α is a parameter larger than zero. The principle of least degeneracy, due to Van Dyke [3], states that the inner problem must include in the first approximation any essential elements omitted in the first outer solution. As an application of the principle, at least one term of the right-hand side in equation (13) should be involved in the inner expansion. Thus α must be 2 so that the first-order inner expansion from equation (13) can be formulated by

$$Pr\, f_{\eta} \Theta_X = \Theta_{XX}. \tag{17}$$

The solution, $\Theta = C_1 \exp(Pr\, f_{\eta} X)$, where C_1 is an arbitrary constant, exponentially vanishes as $X \to -\infty$, but increases as $X \to \infty$, which does not satisfy the matched condition. In other words, equations (15) and (17) cannot be matched in a public regime. It is obvious that although the principle of least degeneracy is a necessary and sufficient condition in the first-order inner expansion for ordinary differential equations, it is not enough for elliptic-to-parabolic equations where the principle can be treated as a necessary but not sufficient condition. The reason is that the principle only explains how to treat the lost terms in the outer expansion, but it is vague about which other terms of the outer expansion to retain in the inner expansion. The new principle, introduced here, states that both of the highest derivatives and at least another term in the elliptic-to-parabolic equation (13) should be kept in the inner expansion for solving elliptic-to-parabolic equations. Therefore the two independent variables in the equation must be stretched at the same time. The physical explanation is that although the thickness of the thermal boundary layer is very small, the thickness of the boundary layer near the leading-edge is much smaller so that as x is stretched, the other variable η should also be enlarged. As an example, we assume that two independent variables must be stretched, that is, $x = \varepsilon^{\alpha} X \sqrt{(2x_0)}$ and $\eta = \varepsilon^{\beta} Y$ where α, $\beta > 0$. By using these relations and Weyl's expansion (6), equation (13) can be expressed in terms of two new variables

$$-bY\hat{\Theta}_X \varepsilon^{3\beta-\alpha} + \hat{\Theta}_{YY} = -\hat{\Theta}_{XX}\varepsilon^{2-2\alpha+2\beta} + O(\varepsilon) \tag{18}$$

where $b = 2D_0\sqrt{(2x_0)}Pr = 0.66411\sqrt{x_0}\,Pr$ and $\hat{\Theta} = \hat{\Theta}(X, Y)$ which stands for an inner function. If $\alpha \leqslant \beta$, the term $\hat{\Theta}_{XX}$ will be canceled which violates the principle of least degeneracy. Therefore, α must be greater than β. With our new principle, let the indices of equation (18) both be zero. Two algebraic equations are immediately obtained

$$3\beta - \alpha = 0; \quad 2 - 2\alpha + 2\beta = 0. \tag{19}$$

A straight-forward calculation shows that the indices are $\alpha = 3/2$ and $\beta = 1/2$. The resulting first-order inner expansion from equation (18) is

$$\hat{\Theta}_{XX} + \hat{\Theta}_{YY} - bY\hat{\Theta}_X = 0. \tag{20}$$

Equation (20) has obvious physical significance. The first two terms represent heat diffusion near the leading-edge. The last term denotes heat convection. In this region the velocity field varies *linearly* with the distance from the surface of the plate. The form of equation (20) is similar to the results derived by Lin [19] and Ackerberg *et al.* [20] where they considered shear flow over a plate. However, equation (20) is expressed in terms of the transformed variables (X, Y) which is different from shear flow in the Cartesian coordinate system (x, y) since the transformation, $x = \varepsilon^{3/2} X\sqrt{(2x_0)}$ and $y = \varepsilon^{3/2} Y\sqrt{(2(x+x_0))}$, is nonlinear.

The differential equations governing energy transfer in the different domains can be found in Fig. 2. Since the neighborhood about the point $x = 0$ is inside of the boundarys $x = -\infty$ and ∞, it can be defined as an internal boundary layer. Equation (20) also can be named the *internal boundary layer equation*. Table 1 summarizes the types of expansions which have been utilized to solve equations (7) and (13). Notice that, whereas previous methods treated elliptic equations, this method first transforms the equation to an elliptic-to-parabolic one. Then the inner expansion of the elliptic-to-parabolic equation will degenerate into an elliptic one again. However, the degeneration will simplify the orginal equation, which has power series coefficients, into one with a linear coefficient, equation (20). Eckhaus [15] has noted that the terminology of inner and outer expansion is sometimes confusing due to its connotation from pure mathematics. Since the terminology is applied extensively in fluid mechanics and heat transfer, however, the terms inner and outer expansion are used here. Note also that the boundary layer equation (15) is an inner expansion of the elliptic equation and an outer expansion of the elliptic-to-parabolic equation. Since the internal boundary layer equation (20) is an inner expansion of the elliptic-to-parabolic equation, it is obvious why it also can be called a boundary layer within a boundary layer.

3. SOLUTION OF THE BOUNDARY LAYER EQUATION (15)

Since the outer expansion of the elliptic equation (7) is identical to zero, the boundary conditions for equation (15) are obtained directly from conditions (8)–(11)

$$\Theta_1(x, \eta) = H(x), \quad \eta = 0; \tag{21}$$

$$\Theta_1(x, \eta) = 0, \quad \eta \to \infty; \tag{22}$$

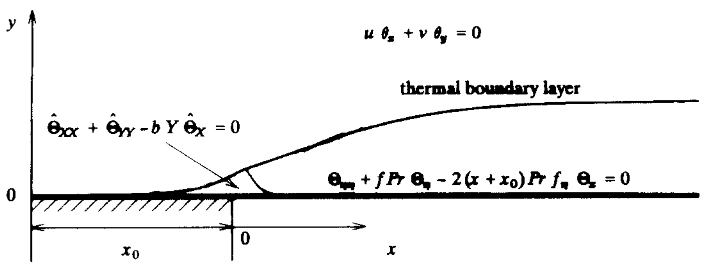

FIG. 2. Governing differential equations in the different thermal domains.

$$\Theta_1(x,y) = 0, \qquad x \to -\infty; \tag{23}$$

$$\Theta_{1_x}(x,y) = 0, \qquad x \to \infty;\ y > 0. \tag{24}$$

The governing equation (15) is parabolic in the x-direction and therefore one of the boundary conditions (23) or (24) must be dropped. After a second-stage similarity transformation converts the equation into a set of ordinary differential equations of second-order in terms of a new independent variable, ζ, the remaining boundary condition (23) or (24) will also be neglected. In fact, all similarity transformations from parabolic equations to ordinary differential equations involve the loss of one boundary condition. Fortunately, the boundary condition will be satisfied automatically after the solution is found for most boundary-value problems. We will show this conclusion later. The proposed transform is defined by

$$\zeta = \eta(x_0/x)^{1/3}. \tag{25}$$

Equation (15) can be expressed in terms of x and ζ

$$Pr^{-1}(x_0/x)^{1/3}\Theta_{1_{\zeta\zeta}} + f\Theta_{1_\zeta} = 2(1+x_0/x)f_\zeta(x\Theta_{1_x} - \Theta_{1_\zeta}/3). \tag{26}$$

Inserting expression (6) for f in terms of the new coordinates (x,ζ) into the previous equation gives

$$Pr^{-1}\Theta_{1_{\zeta\zeta}} + \sum_{n=0}^{\infty}(-1)^n D_n\zeta^{3n+2}\left(\frac{x}{x_0}\right)^{n+1}\Theta_{1_\zeta} = 2\left(\frac{x}{x_0}+1\right)(x\Theta_{1_x} - \Theta_{1_\zeta}\zeta/3)\sum_{n=0}^{\infty}(-1)^n(3n+2) \times D_n\zeta^{3n+1}\left(\frac{x}{x_0}\right)^n \tag{27}$$

which can be solved by a series expansion. Suppose that the power series has the form

$$\Theta_1(x,\zeta) = \sum_{j=0}^{\infty}\theta_j(x/x_0)^j \tag{28}$$

where θ_j is a function of the single variable, ζ. Substituting this solution into equation (27), and equating the coefficients of the homogeneous powers of x, a set of ordinary differential equations results. The equation corresponding to the jth power of x is

$$Pr^{-1}\theta_{j\zeta\zeta} + (4D_0\zeta^2/3)\theta_{j\zeta} - 4D_0\zeta j\theta_j = \sum_{k=0}^{j-2}(-1)^k(j-1-k)\theta_{j-1-k}\zeta^{3k+1}[(6k+4)D_k - \zeta^3(6k+10)D_{k+1}] + \sum_{k=0}^{j-1}(-1)^k\theta_{j-1-k\zeta}\zeta^{3k+2} \times [(2k+10/3)D_{k+1}\zeta^3 - (2k+7/3)D_k]. \tag{29}$$

Considering the regime of $x > 0$, boundary conditions (21) and (22) can be simplified into

$$\theta_0(x,0) = 1;\quad \theta_0(x,\infty) = \theta_j(x,0) = \theta_j(x,\infty) = 0; \quad j \geq 1. \tag{30}$$

Boundary conditions (23) and (24) along the x-direction have been dropped. When $j = 0$, the solution of equation (29), θ_0, which satisfies boundary conditions (30) has the closed form

$$\theta_0 = E\int_\zeta^\infty \exp(-4\zeta^3\,Pr\,D_0/3)\,d\zeta$$

where

Table 1. Types of expansions for the thermal energy equation

Eckhaus [15]	Van Dyke [3]	Ma *et al.* (this paper)
Elliptic equation (7)	Elliptic equation (7)	Elliptic-to-parabolic (13)
Regular expansion (12)	Outer expansion inviscid flow (12)	
Local expansion intermediate boundary layer	Inner expansion boundary layer (15)	Outer expansion boundary layer (15)
Local expansion internal boundary layer		Inner expansion internal boundary layer (20)

$$E = 1\bigg/\int_0^\infty \exp(-4\zeta^3\,Pr\,D_0/3)\,d\zeta = 0.527226\,\mathrm{Pr}^{1/3}. \tag{31}$$

When $j \geqslant 1$, the solution θ_j can be expressed in the form of a power series

$$\theta_j = E\sum_{i=0}^{2j-1} C_{j,i}\zeta^{3i+1}\exp(-4\zeta^3\,Pr\,D_0/9) \tag{32}$$

where $C_{j,i}$ are a set of undetermined constants. Substituting solution (32) into the ordinary differential equation (29) a set of algebraic equations can be found

$$\begin{aligned}
&(3/Pr)\sum_{i=0}^{2j-2} C_{j,i+1}\zeta^{3i+2}(3i+4)(i+1)\\
&-4D_0\sum_{i=0}^{2j-1} C_{j,i}\zeta^{3i+2}(j+i+1)\\
&=(-1)^j\zeta^{3j-1}[(2j+4/3)D_j\zeta^3-(2j+1/3)D_{j-1}]\\
&+\sum_{k=0}^{j-2}\{(-1)^k(j-k-1)\zeta^{3k+2}[(6k+4)D_k\\
&-\zeta^3(6k+10)D_{k+1}]\sum_{i=0}^{2(j-k)-3} C_{j-k-1,i}\zeta^{3i}\}\\
&+\sum_{k=0}^{j-2}\{(-1)^k\zeta^{3k+2}[(2k+10/3)D_{k+1}\zeta^3\\
&-(2k+7/3)D_k]\sum_{i=0}^{2(j-k)-3} C_{j-k-1,i}\zeta^{3i}[(3i+1)\\
&-4Pr\,D_0\zeta^3/3]\}.
\end{aligned} \tag{33}$$

Comparing coefficients in front of powers of ζ, the $C_{j,i}$ can be obtained immediately with a FORTRAN program of 30 statements. The temperature field from equations (28) and (32) is

$$\Theta_1(x,\zeta) = E\left[\int_\zeta^\infty \exp(-4\zeta^3\,Pr\,D_0/3)\,d\zeta + \sum_{j=1}^{\infty}\sum_{i=0}^{2j-1} C_{j,i}\zeta^{3i+1}\exp(-4\zeta^3\,Pr\,D_0/9)(x/x_0)^j\right]. \tag{34}$$

The local Nusselt number can then be calculated by

$$\begin{aligned}
Nu_{x_0+x} &= -(x_0+x)\zeta_y\Theta_{1\zeta}|_{\zeta=0}\\
&= -0.3728\,Re_{x+x_0}^{1/2}(Pr\,x_0)^{1/3}\sum_{j=0}^{\infty} C_{j,0}(x/x_0)^j
\end{aligned} \tag{35}$$

where the coefficient, $C_{0,0}$ is defined to be -1. The coefficients, $C_{j,0}$ for various Prandtl numbers have been listed in Table 2. The series solution (35) is divergent for $x/x_0 > x^*$, where x^* denotes the radius of convergence of the series which can be determined by means of a Domb–Sykes plot [21]. However, a simpler rule applied here is that $x^* = Pr$ for $Pr \leqslant 0.5$ and $x^* = 1$ as $Pr > 0.5$. In order to improve this type of series, Van Dyke [21], Aziz and Na [22] present many techniques, such as Euler transformations, extraction of singularities and Shanks transformations. Computational experience shows that a better technique is to move the summation in equation (35) into the cubic root before utilizing a Euler or Shanks transformation. With a Euler transformation, however, the local Nusselt number in equation (35) can be expressed by the explicit formula

$$Nu_{x_0+x} = 0.3728\,Re_{x_0+x}^{1/2}\left[\frac{Pr}{x^*\hat{x}}\sum_{j=0}^{\infty} B_j\hat{x}^j\right]^{1/3}$$

where

$$\hat{x} = \frac{x}{x+x^*x_0}. \tag{36}$$

Table 2 lists the coefficients, B_j for various Prandtl numbers. For comparison of the methods, a new function from equation (36) is defined by

$$\begin{aligned}
\phi_x &= \frac{Nu_{x_0+x}}{Re_{x_0+x}^{1/2}} = 0.3728\left[\frac{Pr}{x^*\hat{x}}\sum_{j=0}^{\infty} B_j\hat{x}^j\right]^{1/3};\\
\phi_\infty &= \frac{Nu_{x_0+x}}{Re_{x_0+x}^{1/2}} = \lim_{x\to\infty} 0.3728\left[\frac{Pr}{x^*\hat{x}}\sum_{j=0}^{\infty} B_j\hat{x}^j\right]^{1/3}.
\end{aligned} \tag{37}$$

Of course, ϕ_∞ is identical to the solution of a uniformly heated plate, i.e. a self-similar flow which can be obtained exactly with a Runge–Kutta algorithm. Taking x_0 as a unit length, Table 3 lists a summary of the results of ϕ_∞ from these methods and von Kármán integral methods which is

$$\begin{aligned}
\phi_x^{\text{int}} &= \frac{Nu_{x_0+x}}{Re_{x_0+x}^{1/2}} = 0.3313\,Pr^{1/3}\left[1-\left(\frac{x_0}{x_0+x}\right)^{3/4}\right]^{-1/3};\\
\phi_\infty^{\text{int}} &= \frac{Nu_{x_0+x}}{Re_{x_0+x}^{1/2}} = 0.3313\,Pr^{1/3}.
\end{aligned} \tag{38}$$

It should be noted that the error increases with decreasing Prandtl number for differential solutions. The reason, as shown by Chao and Cheema [8] is that Weyl's expansion (6) has a finite radius of convergence. However, the series expansion in this paper is successful for $0.1 \leqslant Pr \leqslant 100$ since the maximum of the errors is less than 2%. As reported by Chao and Cheema in the same paper, the errors for ϕ_∞, reported in Table 3, are the upper bound of error so that we can predict that the error from ϕ_x will decrease when x approaches the leading-edge. The resulting profile, ϕ_x from integral and differential methods are plotted in Figs. 3–5 corresponding to $Pr = 0.1$, 1 and 100, respectively.

The Taylor expansion of the integral solution (38) is obtained near the leading-edge, $\phi_x^{\text{int}} = 0.3646(Pr\,x_0/x)^{1/3}+O(x^{2/3})$. Comparing this result and the first term of the series (35), the relative error is about 2% which is independent of Prandtl numbers. It is not difficult to conclude from this analysis and the results in Table 3 that Nusselt numbers from the integral method are accurate to about 2% for non-similarity flows in the region $0.5 \leqslant Pr \leqslant 100$. However, when boundary layer theory breaks down,

Table 2. Coefficients of nonsimilarity boundary layer solutions (35) and (36)

j	$Pr = 0.1$ $-C_{j,0}$	$Pr = 0.1$ B_j	$Pr = 1$ $-C_{j,0}$	$Pr = 1$ B_j	$Pr = 100$ $-C_{j,0}$	$Pr = 100$ B_j
0	0.10000E+01	0.10000E+01	0.10000E+01	0.10000E+01	0.10000E+01	0.10000E+01
1	0.15278E+00	−0.95417E+00	0.27778E+00	−0.16667E+00	0.29153E+00	−0.12542E+00
2	0.15432E−01	0.11632E−02	−0.90679E−01	−0.40556E−01	−0.97162E−01	−0.36521E−01
3	−0.31553E−01	0.10862E−02	0.50326E−01	−0.19275E−01	0.54482E−01	−0.18251E−01
4	−0.71817E−02	0.10044E−02	−0.33695E−01	−0.11524E−01	−0.36693E−01	−0.11214E−01
5	0.67127E−01	0.91965E−03	0.24859E−01	−0.77659E−02	0.27169E−01	−0.76960E−02
6	−0.36490E−01	0.83374E−03	−0.19461E−01	−0.56347E−02	−0.21321E−01	−0.56606E−02
7	−0.23113E+00	0.74845E−03	0.15858E−01	−0.42994E−02	0.17401E−01	−0.43661E−02
8	0.35397E+00	0.66533E−03	−0.13301E−01	−0.34025E−02	−0.14610E−01	−0.34865E−02
9	0.15261E+01	0.58570E−03	0.11401E−01	−0.27685E−02	0.12532E−01	−0.28587E−02
10	−0.48455E+01	0.51061E−03	−0.99400E−02	−0.23023E−02	−0.10931E−01	−0.23932E−02
11	−0.14499E+02	0.44084E−03	0.87852E−02	−0.19487E−02	0.96633E−02	−0.20376E−02
12	0.88556E+02	0.37690E−03	−0.78519E−02	−0.16734E−02	−0.86376E−02	−0.17591E−02
13	0.16990E+03	0.31904E−03	0.70836E−02	−0.14547E−02	0.77923E−02	−0.15365E−02
14	−0.21214E+04	0.26728E−03	−0.64412E−02	−0.12777E−02	−0.70849E−02	−0.13554E−02
15	−0.16610E+04	0.22146E−03	0.58970E−02	−0.11323E−02	0.64853E−02	−0.12060E−02
16	0.64360E+05	0.18128E−03	−0.54306E−02	−0.10112E−02	−0.59711E−02	−0.10811E−02
17	−0.35328E+05	0.14637E−03	0.50270E−02	−0.90932E−03	0.55258E−02	−0.97557E−03
18	−0.23933E+07	0.11625E−03	−0.46746E−02	−0.82264E−03	−0.51369E−02	−0.88544E−03
19	0.52959E+07	0.90470E−04	0.43646E−02	−0.74824E−03	0.47946E−02	−0.80781E−03
20	0.10571E+09	0.68534E−04	−0.40899E−02	−0.68387E−03	−0.44913E−02	−0.74044E−03
21	−0.46675E+09	0.49986E−04	0.38450E−02	−0.62777E−03	0.42208E−02	−0.68154E−03
22	−0.53630E+10	0.34392E−04	−0.36255E−02	−0.57856E−03	−0.39783E−02	−0.62972E−03
23	0.40518E+11	0.21353E−04	0.34276E−02	−0.53513E−03	0.37598E−02	−0.58388E−03
24	0.29928E+12	0.10510E−04	−0.32486E−02	−0.49660E−03	−0.35619E−02	−0.54309E−03
25	−0.37631E+13	0.15459E−05	0.30858E−02	−0.46225E−03	0.33820E−02	−0.50664E−03
26	−0.17014E+14	−0.58214E−05	−0.29372E−02	−0.43147E−03	−0.32179E−02	−0.47391E−03
27	0.38185E+15	−0.11836E−04	0.28012E−02	−0.40378E−03	0.30675E−02	−0.44440E−03
28	0.78094E+15	−0.16709E−04	−0.26761E−02	−0.37878E−03	−0.29293E−02	−0.41769E−03
29	−0.42461E+17	−0.20621E−04	0.25609E−02	−0.35612E−03	0.28020E−02	−0.39343E−03
30	0.17915E+17	−0.23729E−04	−0.24543E−02	−0.33551E−03	−0.26842E−02	−0.37133E−03
31	0.51561E+19	−0.26164E−04	0.23556E−02	−0.31671E−03	0.25751E−02	−0.35112E−03
32	−0.15929E+20	−0.28037E−04	−0.22638E−02	−0.29950E−03	−0.24737E−02	−0.33260E−03
33	−0.67071E+21	−0.29444E−04	0.21783E−02	−0.28371E−03	0.23793E−02	−0.31558E−03
34	0.43691E+22	−0.30465E−04	−0.20986E−02	−0.26919E−03	−0.22911E−02	−0.29989E−03
35	0.97419E+23	−0.31165E−04	0.20239E−02	−0.25580E−03	0.22087E−02	−0.28540E−03

integral solutions will lead to a tremendous error which is reported in next section.

4. SOLUTION OF THE INTERNAL BOUNDARY LAYER EQUATION (20)

The boundary conditions of equation (20) can be constructed with Van Dyke's asymptotic matching principle: the 1-term inner expansion (of the 1-term outer expansion) is equal to the 1-term outer expansion (of the 1-term inner expansion). However, the outer expansion of the elliptic-to-parabolic equation should be applied corresponding to the inner expansion (20) as the inner variable, X approaches infinity. The reason is that the internal boundary layer equation (20) governs the majority of the negative x-axis including the leading-edge when η is very small and the boundary layer equation governs the entire positive x-axis excluding the leading-edge when η is very small. Therefore, matching along the x-direction should be performed with the boundary layer solution (34)

$$\hat{\Theta}(\infty, Y) = \Theta_1(0, y) = 0. \quad (39)$$

On the other hand, the outer expansion of the elliptic equation should be applied corresponding to the inner expansion (20) when the inner variable Y approaches

Table 3. Similarity boundary layer solution, $\phi_x = Nu_{x_0+x}/Re_{x_0+x}^{1/2}$

Pr	0.1	0.72	1	100
Exact	0.1400	0.2956	0.3321	1.572
Integral method (38)	0.1538	0.2970	0.3313	1.538
Error	9.86%	0.47%	−0.21%	−2.16%
Euler transform (37)	0.1423	0.2980	0.3339	1.581
Error	1.64%	0.81%	0.54%	0.57%
Shanks transform (35)	0.1423	0.2966	0.3323	1.574
Error	1.64%	0.34%	0.06%	0.13%

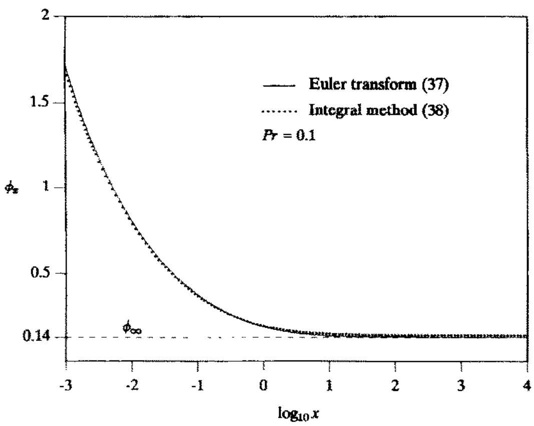

FIG. 3. Nonsimilarity boundary layer solution, $\phi_x = Nu_{x_0+x}/Re^{1/2}_{x_0+x}$.

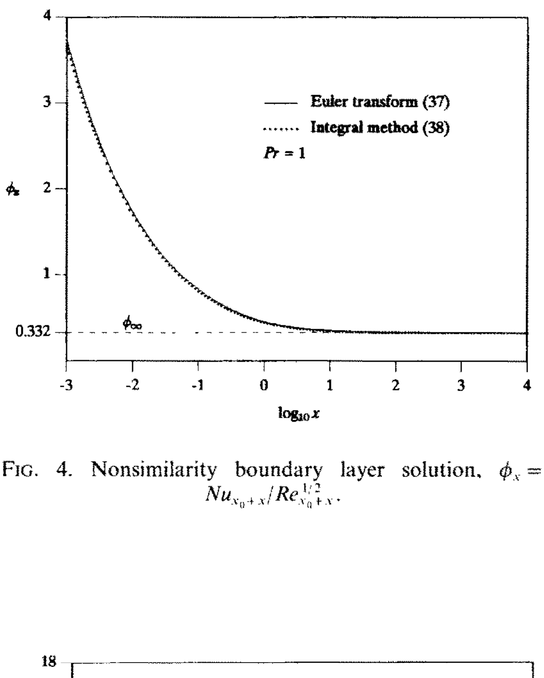

FIG. 4. Nonsimilarity boundary layer solution, $\phi_x = Nu_{x_0+x}/Re^{1/2}_{x_0+x}$.

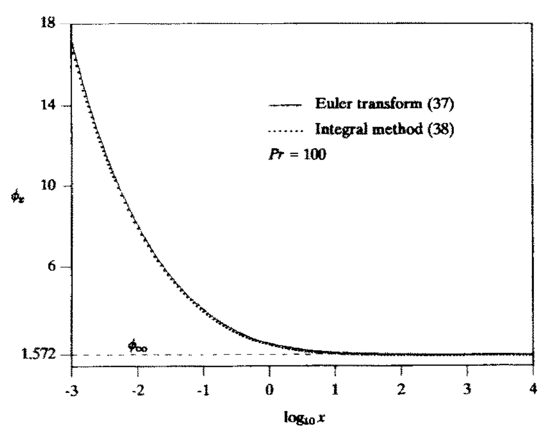

FIG. 5. Nonsimilarity boundary layer solution, $\phi_x = Nu_{x_0+x}/Re^{1/2}_{x_0+x}$.

infinity which is the public regime of both expansions, that is

$$\hat{\Theta}(X, \infty) = \theta(x, 0) = 0. \tag{40}$$

The physical significance of the matched conditions (39) and (40) are that the temperature at these interfaces are continuous. The other two boundary conditions can be obtained from equations (8) and (10)

$$\hat{\Theta}(X, 0) = H(X); \tag{41}$$

$$\hat{\Theta}(-\infty, Y) = 0. \tag{42}$$

With the aid of the Fourier transform defined by

$$F(s, Y) = \frac{1}{\sqrt{(2\pi)}} \int_{-\infty}^{\infty} \hat{\Theta}(X, Y) \exp(sXi)\, dX \tag{43}$$

equation (20) and boundary conditions (40)–(43) can be expressed in terms of s and Y [23]

$$F_{YY} + bs\left(Yi - \frac{s}{b}\right)F = 0 \tag{44}$$

$$F(s, \infty) = 0 \tag{45}$$

$$F(s, 0) = \sqrt{(\pi/2)}\left[\delta(s) + \frac{i}{\pi s}\right] \tag{46}$$

where $\delta(s)$ denotes the Dirac delta function. Equation (44) satisfies boundary conditions (39) and (42). Using substitution of variables, equation (44) can be transformed into a second order ordinary differential equation

$$F_{\xi\xi} - \xi F = 0$$

where

$$\xi = b^{1/3}s^{1/3} \exp(\pi i/2)(Y + is/b). \tag{47}$$

One of the linearly independent solutions of equation (47) may be expressed in terms of an Airy function, Ai or two modified Bessel functions of the first kind with fractional parts $I_{-1/3}$ and $I_{1/3}$, respectively [24]

$$F(s, Y) = M(s)Ai(\eta) = M(s)\tfrac{1}{3}\sqrt{\eta}[I_{-1/3}(\zeta) - I_{1/3}(\zeta)] \tag{48a}$$

where $M(s)$ is an unknown function and

$$\eta = \xi \exp(-2\pi i/3), \quad \zeta = 2\eta^{3/2}/3 \quad \text{if } s > 0. \tag{48b}$$

In fact, s is defined on the entire real-axis, but ξ in equation (47) is a complex independent variable. Therefore solution (48b) represents the case $s > 0$. For the case $s < 0$, it is quite clear that ξ in equation (47) is a conjugate complex number which leads to the conclusion that η in equation (48b) also should be a conjugate variable, that is

$$\eta = \xi \exp(2\pi i/3), \quad \zeta = 2\eta^{3/2}/3 \quad \text{if } s < 0. \tag{48c}$$

Letting $Y \to \infty$ in equation (47), equation (48) can be written as

$$\eta \sim Y \exp(-\pi i/6) \quad \text{and} \quad \zeta \sim Y^{3/2} \exp(-\pi i/4)$$
$$\text{if } s > 0$$

$$\eta \sim Y \exp(\pi i/6) \quad \text{and} \quad \zeta \sim Y^{3/2} \exp(\pi i/4)$$
$$\text{if } s < 0. \tag{49}$$

From these results and asymptotic expansions of the Bessel functions, the boundary condition (45) is satisfied automatically by solution (48). Thus the second linearly independent solution of equation (47) is not required. The boundary condition (46) may be applied to find the unknown function, $M(s)$ in equation (48a). The result is

$$F(s, Y) = N(s, Y)\sqrt{(\pi/2)}\left[\delta(s) + \frac{i}{\pi s}\right] \tag{50a}$$

where

$$N(s, Y) = \frac{Ai[b^{1/3}s^{1/3}\exp(-\pi i/6)(Y + is/b)]}{Ai[s^{4/3}\exp(\pi i/3)/b^{2/3}]}$$
$$\text{if } s > 0 \tag{50b}$$

$$N(s, Y) = \frac{Ai[b^{1/3}s^{1/3}\exp(-5\pi i/6)(Y + is/b)]}{Ai[s^{4/3}\exp(-\pi i/3)/b^{2/3}]}$$
$$\text{if } s < 0. \tag{50c}$$

With inversion of the Fourier transform defined by

$$\hat{\Theta}(X, Y) = \frac{1}{\sqrt{2(\pi)}}\int_{-\infty}^{\infty} F(s, Y)\exp(-sXi)\,\mathrm{d}s \tag{51}$$

the inner expansion can be expressed as

$$\hat{\Theta}(X, Y) = \frac{1}{2}\int_{-\infty}^{\infty} N(s, Y)\left[\delta(s) + \frac{i}{\pi s}\right] \times \exp(-sXi)\,\mathrm{d}s$$
$$= \frac{1}{2} + \frac{i}{2\pi}\int_0^{\infty} \frac{Ai[s^{1/3}\exp(-\pi i/6)(Yb^{1/2} + is)]}{Ai[s^{4/3}\exp(\pi i/3)]} \times \frac{\exp(-sXb^{1/2}i)}{s}\,\mathrm{d}s - \frac{i}{2\pi}\int_0^{\infty} \frac{Ai[s^{1/3}\exp(\pi i/6)(Yb^{1/2} - is)]}{Ai[s^{4/3}\exp(-\pi i/3)]} \times \frac{\exp(sXb^{1/2}i)}{s}\,\mathrm{d}s. \tag{52}$$

In order to obtain the Nusselt number, differentiation of $\hat{\Theta}$ with respect to Y may be performed at $Y = 0$, that is

$$\hat{\Theta}_Y|_{Y=0} = M_1 + M_2$$
$$= \frac{b^{1/2}}{2\pi}\int_0^{\infty} \frac{Ai'[s^{4/3}\exp(\pi i/3)]}{Ai[s^{4/3}\exp(\pi i/3)]} \times \frac{\exp(-sXb^{1/2}i)}{s^{2/3}}\,\mathrm{d}s\exp(\pi i/3) + \frac{b^{1/2}}{2\pi}\int_0^{\infty} \frac{Ai'[s^{4/3}\exp(-\pi i/3)]}{Ai[s^{4/3}\exp(-\pi i/3)]} \times \frac{\exp(sXb^{1/2}i)}{s^{2/3}}\,\mathrm{d}s\exp(-\pi i/3) \tag{53}$$

where Ai' represents the differentiation of Ai. The convergence of the integrations in equation (53) is very slow. However, it may be improved by means of the Cauchy residue theorem and complex variables [23]. According to the definition of the Airy function, its zeros lie on the negative real axis, that is

$$Ai(-s_j) = 0; \quad \text{where} \quad j = 1, 2, 3, \ldots \tag{54}$$

Table 4 lists the first 32 values of s_j found by IMSL [25]. Larger zeros can be obtained by expressing Ai in terms of the asymptotic expansion of Bessel functions of the first kind [24]

$$Ai(-s_j) \sim \tfrac{1}{3}\sqrt{s_j}\left[\cos\left(\frac{2}{3}s_j^{3/2} - \frac{5\pi}{12}\right) + \cos\left(\frac{2}{3}s_j^{3/2} - \frac{\pi}{12}\right) + O(s_j^{-1})\right] = 0. \tag{55}$$

From triangle identities, the solution of equation (55) is found to be

$$s_j \sim (\tfrac{3}{2}j\pi - \tfrac{3}{8}\pi)^{2/3}, \quad \text{as } j \to \infty. \tag{56}$$

When $j = 32$, the result $s_j = 28.1832$ from equation (56) is very close to the value in Table 4. After M_1 in equation (53) for $X < 0$ is expanded into the first quadrature of the complex plane, the integral contour is plotted in Fig. 6. It can be shown that integration along the paths C_R and C_r are equal to zero if $R \to \infty$ and $r \to 0$, respectively. The result around $z_j = \exp(\pi i/2)s_j^{3/4}$ is not equal to zero if $r \to 0$. The application of Cauchy's theorem gives the following formula:

$$M_1 = \frac{b^{1/2}i}{2\pi}\int_0^{\infty} \frac{Ai'(-s)\exp(sXb^{1/2})}{Ai(-s)s^{2/3}}\,\mathrm{d}s + \frac{3b^{1/2}}{8}\sum_{j=1}^{\infty} \frac{\exp(Xs_j^{3/4}b^{1/2})}{s_j^{3/4}}. \tag{57a}$$

The same technique can be applied for M_2 in equation (53). In order to have the integration along the path C_R be zero, the analytic continuation of M_2 is in the fourth quadrature (Fig. 6) where the integration around $z_j = \exp(-\pi i/2)s_j^{3/4}$ is not equal to zero as $r \to 0$. The result is

$$M_2 = -\frac{b^{1/2}i}{2\pi}\int_0^{\infty} \frac{Ai'(-s)\exp(sXb^{1/2})}{Ai(-s)s^{2/3}}\,\mathrm{d}s + \frac{3b^{1/2}}{8}\sum_{j=1}^{\infty} \frac{\exp(Xs_j^{3/4}b^{1/2})}{s_j^{3/4}}. \tag{57b}$$

Substituting expressions (57) into equation (53), a simple solution is found

$$\hat{\Theta}_Y|_{Y=0} = \frac{3b^{1/2}}{4}\sum_{j=1}^{\infty} \frac{\exp(Xs_j^{3/4}b^{1/2})}{s_j^{3/4}}; \quad (X < 0). \tag{58}$$

The situation, $X > 0$ is also similar except that the analytic continuation of M_1 is in the fourth quadrature, but M_2 is in the first quadrature, which leads to

Table 4. Zeros of the Airy function, $Ai(-s_j) = 0$

j	s_j	j	s_j	j	s_j	j	s_j
1	2.33811	2	4.08795	3	5.52056	4	6.78671
5	7.94413	6	9.02265	7	10.0402	8	11.0085
9	11.9360	10	12.8288	11	13.6915	12	14.5278
13	15.3408	14	16.1327	15	16.9056	16	17.6613
17	18.4011	18	19.1264	19	19.8381	20	20.5373
21	21.2248	22	21.9014	23	22.5676	24	23.2242
25	23.8716	26	24.5103	27	25.1408	28	25.7635
29	26.3788	30	26.9870	31	27.5884	32	28.1833

$$M_1 = \frac{b^{1/2}}{2\pi}\int_0^\infty \frac{Ai'[s^{4/3}\exp(-\pi i/3)]}{Ai[s^{4/3}\exp(-\pi i/3)]}\frac{\exp(-sXb^{1/2})}{s^{2/3}}\,ds \times \exp(\pi i/6)$$

$$M_2 = \frac{b^{1/2}}{2\pi}\int_0^\infty \frac{Ai'[s^{4/3}\exp(\pi i/3)]}{Ai[s^{4/3}\exp(\pi i/3)]}\frac{\exp(-sXb^{1/2})}{s^{2/3}}\,ds \times \exp(-\pi i/6). \quad (59)$$

Substituting equation (59) into (53), with a suitable substitution of variables, $\hat{\Theta}_Y$ at the boundary $Y = 0$ is

$$\hat{\Theta}_Y|_{Y=0} = \frac{b^{1/2}}{\pi}\int_0^\infty \frac{Ai'[s^{4/3}]}{Ai[s^{4/3}]}\frac{\exp(-sXb^{1/2}\sqrt{2}/2)}{s^{2/3}} \times \cos(-sXb^{1/2}\sqrt{2}/2+\pi/4)\,ds; \quad (X>0). \quad (60)$$

Although the result is still in the form of an integral, its convergence is exponential. The local Nusselt number, $Nu_{x_0+x} = -(x_0+x)Y_y\hat{\Theta}_Y|_{Y=0}$, can be found from the previous equations, that is

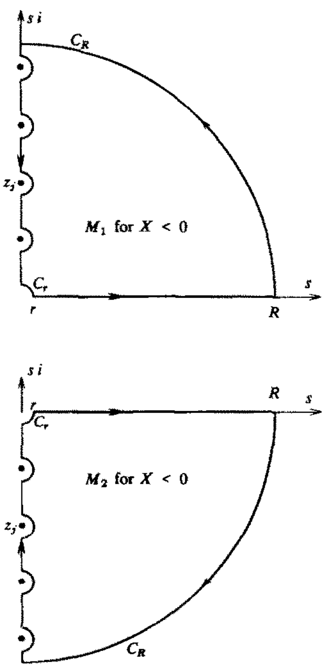

FIG. 6. Contours of integration for the internal boundary layer solution (53).

$$Nu_{x_0+x} = -\sqrt{(x_0+x)}\frac{3b^{1/2}}{4\sqrt{2}}\varepsilon^{-3/2} \times \sum_{j=1}^{\infty}\frac{\exp(Xs_j^{3/4}b^{1/2})}{s_j^{3/4}}; \quad (X<0)$$

$$= -\sqrt{(x_0+x)}\frac{b^{1/2}}{\pi\sqrt{2}}\varepsilon^{-3/2}\int_0^\infty \frac{Ai'(s^{4/3})}{Ai(s^{4/3})} \times \frac{\exp(-sXb^{1/2}\sqrt{2}/2)}{s^{2/3}}\cos\left(\frac{-sXb^{1/2}\sqrt{2}}{2}+\frac{\pi}{4}\right)ds; \quad (X>0). \quad (61)$$

With the value of b in equation (18) and the outer variable $x = \varepsilon^{3/2}X\sqrt{(2x_0)}$, equation (61) can be expressed by

$$Nu_{x_0+x} = -Re_{x_0+x}^{1/2}\left[0.43218\,Re_{x_0}^{1/4}\,Pr^{1/2} \times \sum_{j=1}^{\infty}\frac{\exp(0.57624s_j^{3/4}\,Pr^{1/2}\,Re^{3/4}\,x/x_0^{1/4})}{s_j^{3/4}}\right]; \quad (x<0)$$

$$= -Re_{x_0+x}^{1/2}\left[0.18342\,Re_{x_0}^{1/4}\,Pr^{1/2} \times \int_0^\infty \frac{Ai'(s^{4/3})\exp(w)}{Ai(s^{4/3})\,s^{2/3}}\cos(w+\pi/4)\,ds\right]; \quad (x>0) \quad (62a)$$

where

$$w = -0.40747s\,Pr^{1/2}\,Re^{3/4}\,x/x_0^{1/4}. \quad (62b)$$

Figures 7–9 plot the function, ϕ_x defined by equation (37) for different Prandtl and Reynolds numbers with $x_0 = 1$. The results show that the Nusselt number has an exponential decay along the x-direction. This reflects the effects of the leading-edge of the heated part of the plate. Notice that the Nusselt number approaches infinity when $x \to 0^+$, and minus infinity when $x \to 0^-$. This is similar to the conclusion reported by Arpaci [26] although the problem he investigated is the fully developed laminar flow of a viscous fluid between two parallel plates with a discontinuous plate temperature. Since the maximum

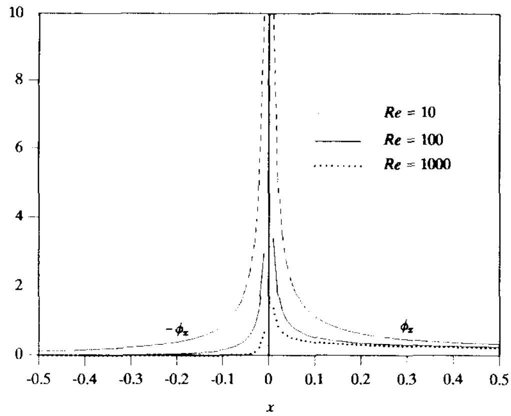

FIG. 7. Internal boundary layer solution for $Pr = 0.1$, $\phi_x = Nu_{x_0+x}/Re_{x_0+x}^{1/2}$.

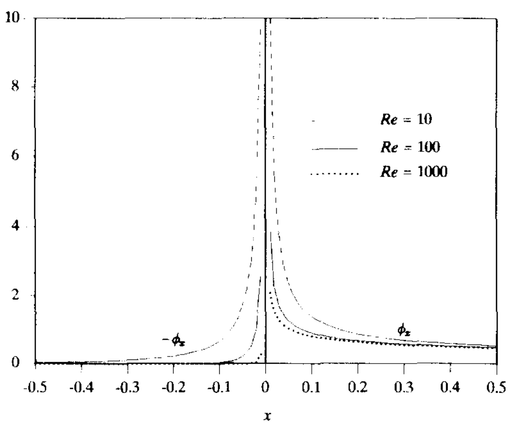

FIG. 8. Internal boundary layer solution for $Pr = 1$, $\phi_x = Nu_{x_0+x}/Re_{x_0+x}^{1/2}$.

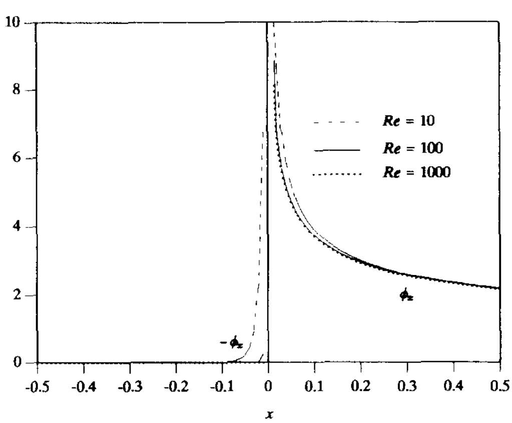

FIG. 9. Internal boundary layer solution for $Pr = 100$, $\phi_x = Nu_{x_0+x}/Re_{x_0+x}^{1/2}$.

value of the temperature is at the plate for $x > 0$ and the minimum value of the temperature is at the plate for $x < 0$, the fluid temperature is obviously between the two. Therefore heat flows into the plate when $x < 0$ so that Nusselt number is less than zero. On the other hand, for $x > 0$, the fluid temperature is less than plate temperature and heat flows from the plate so that the Nusselt number is larger than zero.

5. COMPOSITE EXPANSIONS AND DISCUSSION

The result from boundary layer theory in Section 3 is invalid near the leading-edge of the heated section. Conversely, the internal boundary layer solution in Section 4 is not suitable for the downstream. Since the two expansions have a common region of validity for the case $x > 0$, it is quite easy to construct a single uniformly valid expansion for the elliptic-to-parabolic equation using the concept of composite expansions [3]. The additive composition is used here for its elegance. The rule is that the first-order composite expansion of temperature, θ^c is equal to the sum of the first-order inner and outer expansions corrected by subtracting the inner expansion of the outer expansion , Θ_1^i, which formulates

$$\theta^c = \hat{\Theta} + \Theta_1 - \Theta_1^i \tag{63}$$

where $\hat{\Theta}$ is the inner expansion (51) and Θ_1 is the outer expansion (28). On the other hand, substituting the relation between the inner and outer variables

$$x = \sqrt{(2x_0)}X\varepsilon^{3/2}, \quad \zeta = \frac{Y}{2^{2/3}(Xx_0)^{1/3}} \tag{64}$$

into outer expansion (28), then letting ε approach zero, we have

$$\Theta_1^i = \theta_0(X, Y) = E\int_{\zeta}^{\infty} \exp(-4\zeta^3\, Pr\, D_0/3)\, d\zeta \tag{65}$$

where the lower limit of integration is defined by equation (64). Since the solution of the boundary layer equation is zero as $x < 0$, the first-order composite expansion of temperature is identical to the inner expansion. Taking the derivative of equation (63) with respect to y, utilizing the same definition as in the previous two sections, $\phi_x^c = Nu_{x_0+x}/Re_{x_0+x}^{1/2}$, we find

$$\phi_x^c = -0.18342\, Re_{x_0}^{1/4}\, Pr^{1/2} \times \int_0^{s} \frac{Ai'(s^{4/3})}{Ai(s^{4/3})} \frac{\exp(w)}{s^{2/3}} \cos\left(w + \frac{\pi}{4}\right) ds + 0.3728\left[\left(\frac{Pr}{x^*\hat{x}} \sum_{j=0}^{\infty} B_j \hat{x}^j\right)^{1/3} - \left(\frac{Pr\, x_0}{x}\right)^{1/3}\right] \tag{66}$$

where the integration is the solution (62) of the inner expansion, the series is the solution (36) of the outer expansion and the second term in the brackets is the first term of the outer expansion. When x is very small, the series in equation (66) will be dominated by its first term so that the summation in the bracket approaches zero. Thus the composite expansion, ϕ_x^c degenerates into the first term of equation (66), that is, the inner

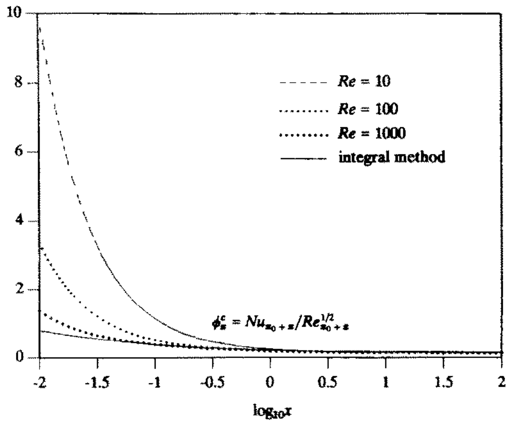

FIG. 10. Comparison between the first-order composite expansion (66) and integral methods (38) for $Pr = 0.1$.

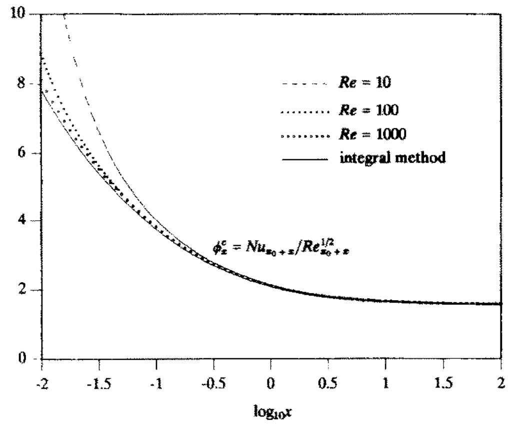

FIG. 12. Comparison between the first-order composite expansion (66) and integral methods (38) for $Pr = 100$.

expansion of the elliptic-to-parabolic equation. In the previous section, we proved that the inner expansion has an exponential decay near the leading-edge. However, if x is very large, it converges as the second term in the bracket of equation (66) which yields the conclusion that ϕ_x^c degenerates into the solution of the outer expansion. The reason for success of the composite expansion is based on the application of Van Dyke's asymptotic matching principle in Section 4.

Results from the first-order composite expansion (66) and integral methods have been plotted in Figs. 10–12. Table 5 also lists some numerical comparisons. From these results, it is obvious that if the length of the heated part is small enough, for instance, $x = 0.01$, the boundary layer solution has a very large error. For example, when $Pr = 0.1$, the ratio $\phi_x^c/\phi_x^{\text{int}}$ is 1.75 even though the flow has a high Reynolds number, 1000. The other interesting phenomenon is that the error decreases with increasing Prandtl number. It should be noted that all of the results from the proposed method are larger than predictions from boundary layer theory. The reason is that the axial diffusion augments the heat transfer. Consequently, the Nusselt number is larger.

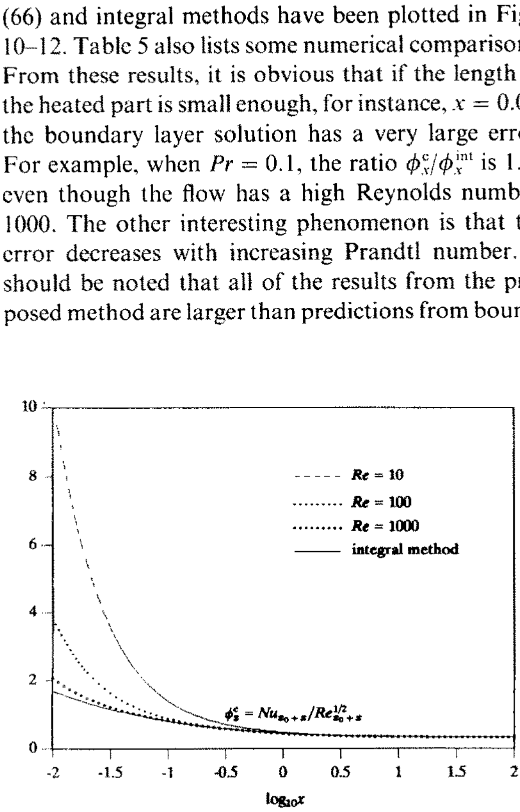

FIG. 11. Comparison between the first-order composite expansion (66) and integral methods (38) for $Pr = 1$.

Considering that the integral method is accurate to about 2% in Section 3, equation (66) has another simpler form

$$\phi_x^c = -0.1834\, Re_{x_0}^{1/4}\, Pr^{1/2} \int_0^\infty \frac{Ai'(s^{4/3})}{Ai(s^{4/3})}\,\frac{\exp(w)}{s^{2/3}} \times \cos\left(w+\frac{\pi}{4}\right) ds + Pr^{1/3}\left\{0.3313\left[1-\left(\frac{x_0}{x_0+x}\right)^{3/4}\right]^{-1/3} - 0.3646\left(\frac{x_0}{x}\right)^{1/3}\right\}. \quad (67)$$

This expression is applicable for $0.5 < Pr < 100$. With the principle of superposition, it is easy to find the local Nusselt number for finite heated sections with unheated starting and ending lengths. If the length of the heated section is l, the x in the first expression of equation (62a) must be changed into $x-l$; x_0 into x_0+l and the negative sign into positive which specifies that heat flows from the plate. The expression represents the effects of the trailing edge of the heated section. The combination of the result and equation (66) yields

$$\phi_x^c = -0.1834\, Re_{x_0}^{1/4}\, Pr^{1/2} \int_0^\infty \frac{Ai'(s^{4/3})}{Ai(s^{4/3})}\,\frac{\exp(w)}{s^{2/3}} \times \cos\left(w+\frac{\pi}{4}\right) ds + 0.3728\left[\left(\frac{Pr}{x^*\hat{x}}\sum_{j=0}^{\infty} B_j \hat{x}^j\right)^{1/3} - \left(\frac{Pr\, x_0}{x}\right)^{1/3}\right] + 0.4322\, Re_{x_0+l}^{1/4}\, Pr^{1/2} \times \sum_{j=1}^{\infty} \frac{\exp[0.5762 s_j^{3/4}\, Pr^{1/2}\, Re^{3/4}\,(x-l)/(x_0+l)^{1/4}]}{s_j^{3/4}};$$

$$(0 \leqslant x \leqslant l). \quad (68)$$

Unfortunately, the integration of equation (66) or (68)

Table 5. Comparison between the first-order composite expansion (66) and integral methods (38)

	$Pr = 0.1$			$Pr = 1$			$Pr = 100$		
x	0.01	0.1	1	0.01	0.1	1	0.01	0.1	1
ϕ_x^c for $Re = 10$	10.190	1.1339	0.2350	10.459	1.4006	0.4727	13.813	4.021	2.128
ϕ_x^c/ϕ_x^{int}	12.9	3.02	1.13	6.16	1.73	1.06	1.75	1.07	1.02
ϕ_x^c for $Re = 100$	3.402	0.5269	0.2029	3.863	0.9088	0.4559	8.895	3.852	2.125
ϕ_x^c/ϕ_x^{int}	4.32	1.41	0.98	2.28	1.13	1.02	1.13	1.03	1.02
ϕ_x^c for $Re = 1000$	1.380	0.3973	0.1992	2.097	0.8337	0.4542	8.144	3.835	2.124
ϕ_x^c/ϕ_x^{int}	1.75	1.06	0.96	1.24	1.03	1.01	1.03	1.02	1.02
Integral, ϕ_x^{int}	0.788	0.3749	0.2078	1.697	0.8078	0.4476	7.879	3.749	2.078

with respect to x diverges in the finite interval $[0, l]$. It is impractical for a real application to have an infinite heat transfer. The reason, as demonstrated in the Appendix, is that the singularity results from the discontinuous boundary condition (8). Boundary layer theory neglects the leading-edge effects so that the average Nusselt number is finite. In other words, there is no singularity without axial conduction. The present method has revealed the entire thermal field. Since the source of the singularity comes from the mathematical model, it is not possible to remove the singularity in higher approximations. In fact, the temperature field is always continuous in practical situations. The gap between the mathematical model and the physical problem can be filled by rebuilding new continuous boundary conditions instead of the Heaviside step function in equation (8). Currently the problem of a small heated section with insulated starting and ending lengths is being investigated.

6. CONCLUSION

The accuracy of integral methods for the non-similarity boundary layer has been reported in Figs. 3–5 where the maximum error is 2% in the region, $0.5 \leqslant Pr \leqslant 100$. Therefore, integral methods are accurate for most applications if and only if the boundary layer theory is valid. If boundary layer theory breaks down in some regions, the new governing equation (20) is derived by means of a generalized principle of least degeneracy. Then the first-order composite expansion is obtained in the sense of additive composition. The comparison between the expansion and integral methods can be found in Figs. 10–12. Numerical results (Table 5) show that the error depends on the Prandtl and Reynolds numbers as well as the length scale of the heated section. It has been shown that a Nusselt number 12.9 times that predicted with an integral technique is possible. Since the axial diffusion augments the heat transfer, the Nusselt number from the proposed method is larger than the prediction using the integral method. The conclusion is that the evaluation of heat transfer from boundary layer theory is more conservative. In order to accurately predict the heat transfer from microstructures, continuous boundary condition must be used. Currently the problem of a small heated section with insulated starting and ending lengths is being investigated.

Acknowledgements—This study was sponsored by the University Research Council and the MINE department at the University of Cincinnati.

REFERENCES

1. B. W. Van Oudheusden and J. H. Huijsing, Integrated flow friction sensor, *Sensors Actuators* **15,** 135–144 (1988).
2. R. J. Moffat and A. Ortega, Direct air-cooling of electronic components, In *Advances in Thermal Modeling of Electronic Components and Systems* (Edited by A. Bar-Cohen and A. D. Kraws). Vol. 1. Hemisphere, New York (1988).
3. M. Van Dyke, *Perturbation Methods in Fluid Mechanics*. Academic, New York (1964). (Annotated Edition (1975).)
4. M. Van Dyke, Higher-order boundary-layer theory, *Ann. Rev. Fluid Mech.* **1,** 265–292 (1969).
5. I. Pop, P. Cheng and T. Le, Leading edge effects on free convection of a Darcian fluid about a semi-infinite vertical plate with uniform heat flux, *Int. J. Heat Mass Transfer* **32,** 493–501 (1989).
6. O. G. Martynenko, A. A. Berezovsky and Yu. A. Sokovishin, Laminar free convection from a vertical plate, *Int. J. Heat Mass Transfer* **27,** 869–881 (1984).
7. L. S. Cheema, Forced convection in laminar boundary layer over wedges of arbitrary temperature and flux distribution, Ph.D. Thesis, University of Illinois at Urbana–Champaign (1970).
8. B. T. Chao and L. S. Cheema, Forced convection in wedge flow with non-isothermal surfaces, *Int. J. Heat Mass Transfer* **14,** 1363–1375 (1971).
9. E. M. Sparrow, H. Quack and C. J. Boerner, Local nonsimilarity boundary layer solutions, *AIAA J.* **8,** 1936–1942 (1970).
10. E. M. Sparrow and H. S. Yu, Local nonsimilarity thermal boundary layer solutions, *J. Heat Transfer* **93,** 328–334 (1971).
11. S. M. Zubair and P. V. Kadaba, Similarity transformations for boundary layer equations in unsteady mixed convection, *Int. Commun. Heat Mass Transfer* **17,** 215–226 (1990).
12. A. Nayfeh, *Perturbation Methods*. Wiley, New York (1973).
13. P. A. Lagerstrom, *Matched Asymptotic Expansions: Ideas and Techniques*, Chap. III. Springer, New York (1988).
14. J. Grasman, On the birth of boundary layers, Thesis, Technical University, Delft Mathematical Center, Amsterdam Tract 36 (1971).

15. W. Eckhaus, *Asymptotic Analysis of Singular Perturbations*, Chap. 7. North-Holland, Amsterdam (1979).
16. C. W. Jones and E. J. Watson, Two-dimensional boundary layers, In *Laminar Boundary Layers* (Edited by L. Rosenhead). Oxford University Press, London (1963).
17. M. Van Dyke, Higher approximation on boundary-layer theory, *J. Fluid Mech.* **14,** 161–177 (1962).
18. Y. H. Kuo, On the flow of an incompressible viscous past a flat plate at moderate Reynolds numbers, *J. Math Phys.* **32,** 83–101 (1953).
19. S. C. Lin, Heat transfer from a small isothermal spanwise strip on an insulated boundary, *J. Heat Transfer* **85,** 230–236 (1963).
20. R. C. Ackerberg, R. D. Patel and S. K. Gupta, The heat/mass transfer to a finite strip at small Péclet numbers, *J. Fluid Mech.* **86,** 49–65 (1978).
21. M. Van Dyke, Analysis and improvement of perturbation series, *Q. J. Mech. Appl. Math.* **27,** 423–440 (1974).
22. A. Aziz and T. Y. Na, *Perturbation Methods in Heat Transfer*. Hemisphere, Washington, DC (1984).
23. L. C. Andrews and B. L. Shivamoggi, *Integral Transforms for Engineers and Applied Mathematicians*. Macmillan, New York (1988).
24. M. Abramowitz and I. A. Stegun, *Handbook of Mathematical Functions*. Dover, New York (1972).
25. *IMSL User's Manual*. IMSL Customer Relations, Houston, Texas (1989).
26. V. S. Arpaci, *Conduction Heat Transfer*. Addison-Wesley, Reading, Massachusetts (1966).
27. I. S. Gradshteyn and I. M. Ryzhik, *Table of Integrals, Series, and Products*. Academic Press, New York (1980).

APPENDIX

The purpose of this appendix is to show the source of the integral singularity. The basic equation examined is for two-dimensional steady-state heat conduction, that is, Laplace's equation

$$\theta_{xx}+\theta_{yy} = 0 \tag{A1}$$

where θ denotes dimensionless temperature. The boundary conditions are defined in the semi-infinite region

$$\theta(-\infty,y) = 0;\quad \theta(\infty,y) = 0;\quad \theta(x,\infty) = 0;$$
$$\theta(x,0) = H(x). \tag{A2}$$

With the aid of the Fourier transform, the solution can be found as

$$\theta = \tfrac{1}{2}+\frac{1}{\pi}\int_0^{\infty}\frac{\exp(-sy)}{s}\sin(sx)\,\mathrm{d}s = \tfrac{1}{2}+\frac{1}{\pi}\tan^{-1}\left(\frac{x}{y}\right). \tag{A3}$$

It is easy to show that solution (A3) satisfies Laplace's equation (A1) and the boundary conditions (A2). Taking the derivative of the solution with respect to y, the gradient of temperature at the plate is

$$\theta_y|_{y=0} = \frac{1}{\pi x}. \tag{A4}$$

At the discontinuity, $\theta_y \to \infty$ as $x \to 0^+$ and $\theta_y \to -\infty$ when $x \to 0^-$ which are similar to the results from Figs. 7–9. On the other hand, the integration from 0 to a finite length with respect to x, say l in equation (A4) shows that the result logarithmically diverges. Using a continuous function $f(x)$ instead of the Heaviside function in equation (A2), the solution under the new boundary conditions is the Poisson integral formula [23]

$$\theta = \frac{y}{\pi}\int_{-\infty}^{\infty}\frac{f(s)\,\mathrm{d}s}{(x-s)^2+y^2};$$
$$\theta_y|_{y=0} = \frac{1}{\pi}\int_{-\infty}^{\infty}\frac{f(s)\,\mathrm{d}s}{(x-s)^2}. \tag{A5}$$

If the function $f(s)$ is defined in an interval, $0 \leqslant s \leqslant l$, the average gradient of temperature at the surface is

$$\frac{1}{l}\int_0^l \theta_y|_{y=0}\,\mathrm{d}x = -\frac{1}{\pi}\int_0^l \frac{f(s)\,\mathrm{d}s}{s(l-s)}. \tag{A6}$$

In order to make the integral of equation (A6) finite, $f(0)$ and $f(l)$ must be zero [27]. Physically, this means that the temperature at the interfaces between the heated and unheated sections of a plate should be continuous.